JOURNAL OF MATERIALS SCIENCE 17 (1982) 701–708

Preparation of a very pure $Fe_2O_3 \cdot x\,H_2O$ gel: some structural and magnetic properties

G. MATZEN, P. POIX
Department Science des Materiaux, E.N.S.C.S., E.R.A. 679 du C.N.R.S., 1 rue Blaise Pascal, B.P. 296/R8, 67008 Strasbourg Cedex, France

A gel of iron (III) oxide hydrate was prepared using the oxidation of a $FeC_2O_4 \cdot 2\,H_2O$ suspension with H_2O_2. Alkaline ions were not employed for the precipitation of the gel and the $C_2O_4^{2-}$ anions which are oxidized to CO_2 disappear rapidly from the solution. A very pure $Fe_2O_3 \cdot xH_2O$ gel is thus obtained. X-ray diffraction and electron microscope studies showed the very little crystalline character of this gel and the different steps of its dehydration and crystallization with increasing temperature. Magnetic measurements at low temperature revealed the remarkable properties of this amorphous $Fe_2O_3 \cdot xH_2O$: superparamagnetism, blocking temperature, T_B, and thermo-remanent magnetization. These properties are characteristic of fine grains and mictomagnetic compounds.

1. Introduction

The ferric oxide α-Fe_2O_3 can be obtained by annealing ferric hydroxide. However, the preparation of $Fe(OH)_3$ by a classical method such as the reaction of a base (e.g., NaOH, KOH, Na_2CO_3) with the solution of a ferric salt does not give a very pure product. The principal reason for this is the adsorption of small quantities of alkaline ions by the obtained hydrate.

An other method of preparation consists of firing certain ferric or ferrous salts in air or oxygen, the purity of the employed salt (a nitrate, sulphate, or carbonate) being important. Fired in air, a ferrous oxalate of high purity gives a good oxide [1]. Nevertheless, because the CO produced during the firing reacts with the oxide, the oxidation step is not certain and the complete elimination of carbon is difficult.

2. Preparation

The method which we have developed provides a ferric hydrate of high purity. This product is obtained by treating an aqueous suspension of $FeC_2O_4 \cdot 2\,H_2O$ with H_2O_2. The first step of the reaction is

$$3\,FeC_2O_4 + 3/2\,H_2O_2 \rightarrow (2\,Fe^{3+} + 3\,C_2O_4^{2-}) + Fe(OH)_3\downarrow. \quad (1)$$

An excess of H_2O_2 leads to a supplementary precipitation of ferric hydroxide if the oxalate solution is sufficiently concentrated:

$$(2\,Fe^{3+} + 3\,C_2O_4^{2-}) + 3\,H_2O_2 \rightarrow 2\,Fe(OH)_3\downarrow + 6\,CO_2\uparrow. \quad (2)$$

The net reaction is

$$3\,FeC_2O_4 + 9/2\,H_2O_2 \rightarrow 3\,Fe(OH)_3\downarrow + 6\,CO_2\uparrow. \quad (3)$$

This method of preparation is particularly interesting: $C_2O_4^{2-}$ is converted to CO_2 and eliminated, and the introduction of an alkaline cation is avoided. The amorphous $Fe_2O_3 \cdot xH_2O$ which is obtained is free from impurities and can be transformed into very pure Fe_2O_3 or Fe. We have studied the structural and magnetic properties of the iron oxide hydrate which appears during the first step of the reaction.

3. Structural properties of the $Fe_2O_3 \cdot xH_2O$ gel

The ferric oxide hydrate prepared from an aqueous suspension at about 50° C was studied after drying at 100° C. The formula $Fe(OH)_3$ is a simplified expression that we have employed for the chemical equations; in fact, the proportion of water contained in the $Fe_2O_3 \cdot xH_2O$ gels varies with the method of preparation. It depends essentially on the temperature and the pH of the solution in

0022–2461/82/030701–08\$03.46/0

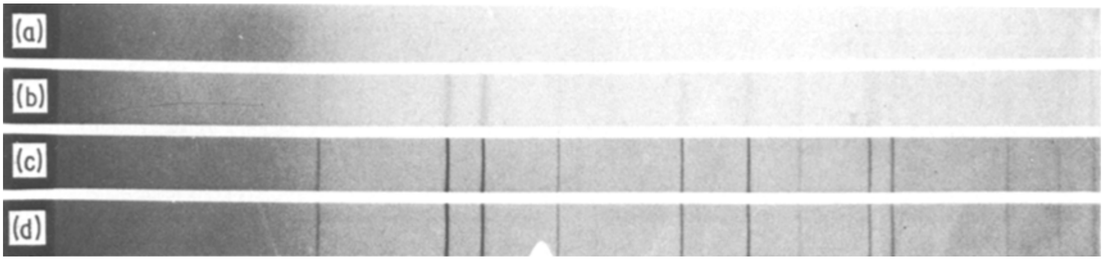

Figure 1 X-ray diffraction patterns of (a) ferric oxide hydrate dried at 100° C, (b) α-Fe_2O_3 obtained from the ferric oxide hydrate (350° C, 4 h), (c) α-Fe_2O_3 obtained from the ferric oxide hydrate (900° C, 2 h), (d) pure commercial iron (III) oxide.

which the hydrate is precipitated and on the temperature used during the drying. Glemser [2] studied a hydroxide of composition $Fe(OH)_3$. Van der Giessen [3] prepared an oxide hydrate having the formula $Fe_2O_3 \cdot 1.2\,H_2O$ and giving a Debye–Scherrer diagram with several broad and weak lines. The iron (III) oxide hydrate we have obtained with our method of preparation has the approximate formula $Fe_2O_3 \cdot 2.4\,H_2O$, as determined from the measurement of the weight loss (about 21%) resulting from annealing for 2 h at 900° C. A thermogravimetric analysis confirmed this determination.

Electron diffraction studies indicate the light crystalline character of the hydrate gels [4]. These gels often correspond in fact to agglomerates of extremely fine particles which are poorly crystallized. The gel of ferric hydroxide we have prepared seems to be amorphous when examined by X-ray diffraction: no line can be seen in the resulting pattern (see Fig. 1a). On the other hand, diffraction circles can be seen in the electron diffraction patterns (see Fig. 2c); these are relatively broad and weak, but they indicate a certain degree of crystallinity. Fig. 2a and b shows agglomerates of fine particles. Fig. 2b allows us to estimate the particle size to be less than 2 nm.

4. Dehydration and crystallization

The dehydration of the hydroxide is practically complete at 250° C as it is shown by thermogra-

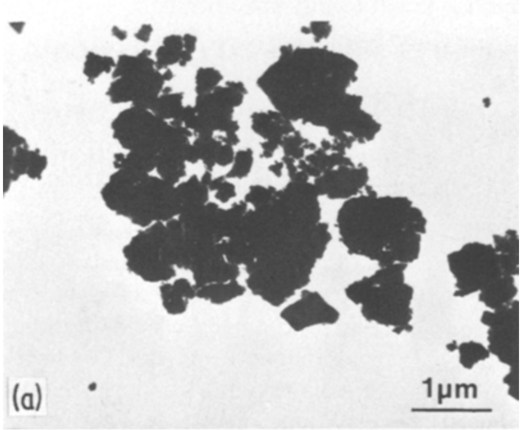

Figure 2 (a) and (b) Transmission electron electron micrographs and (c) electron diffraction pattern of ferric oxide hydrate dried at 100° C.

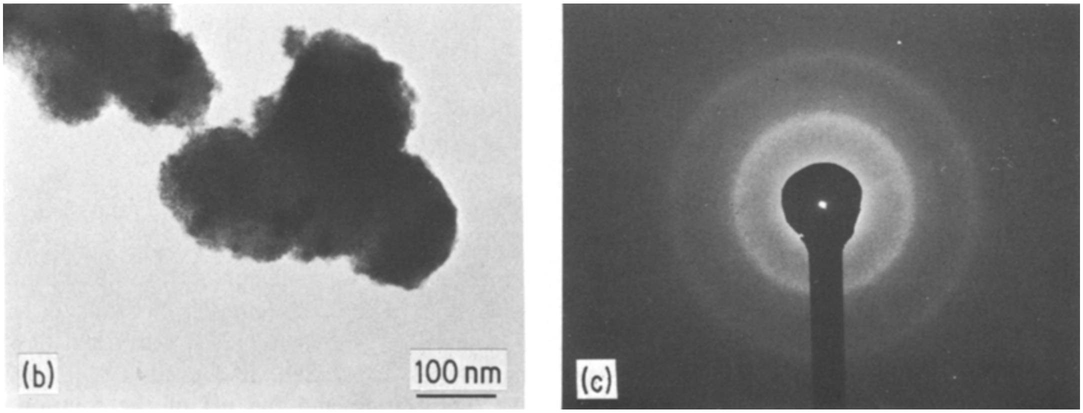

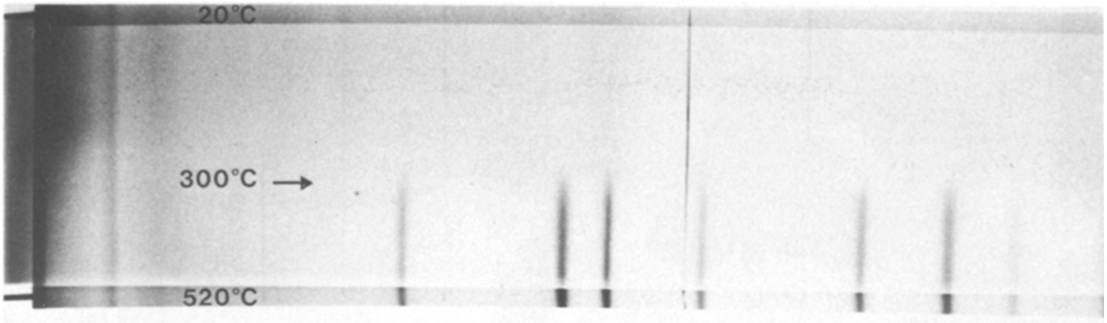

Figure 3 X-ray diffraction pattern (20 to 520° C) of ferric oxide hydrate.

vimetry. An X-ray diffraction study with temperature (see Fig. 3) shows the obvious crystallization of α-Fe_2O_3 after this dehydration at 300° C. A sample of the hydrate was annealed at 350° C for 4 h. The lines of α-Fe_2O_3 appear on the corresponding X-ray diffraction pattern (Fig. 1b). They are relatively broad denoting the still very small size of the crystals. The electron diffraction pattern of these crystals (Fig. 4c) shows punctuated circles due to the limited number of crystals involved in the exposure. This crystalline character is much more obvious than that obtained for the gel of the hydroxide; this correlates very well with the formation of an X-ray diffraction pattern. In addition, Fig. 4b confirms very clearly the enhanced size of the crystals as compared to the hydroxide gel particles. Indeed, the particles of α-Fe_2O_3 have sizes between 10 and 20 nm.

Iron oxides are very much studied at present because of their applications in, for example, the technology of magnetic tapes. In this connection, researchers have especially studied the influence of size on the crystallographical [5] and magnetic [6] properties of particles of γ-Fe_2O_3. The sizes of the studied crystallites are usually in the 10 to 100 nm range. So, the ferric oxide hydrate which obtained could be used, for example, in preparing fine γ-Fe_2O_3 grains of high purity. A possible sequence of reactions is:

$$Fe_2O_3 \cdot 2.4H_2O \rightarrow \alpha\text{-}Fe_2O_3 \text{ (annealing in air, } 350^\circ\text{ C, 1 h)}$$

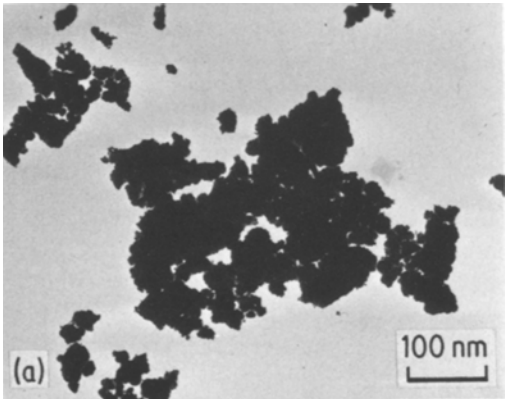

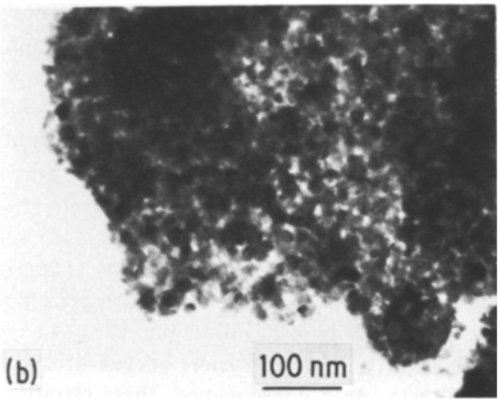

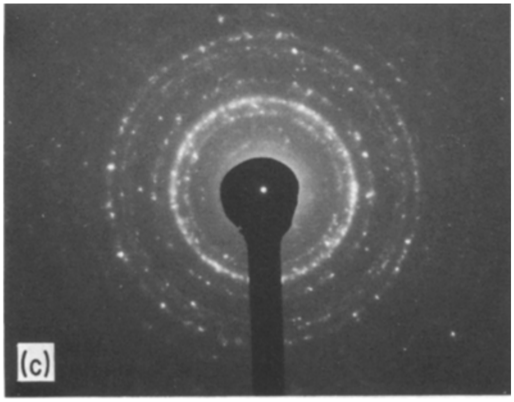

Figure 4 (a) and (b) Transmission electron micrographs and (c) electron diffraction pattern of α-Fe_2O_3 obtained from the ferric oxide hydrate dried at 350° C for 4 h.

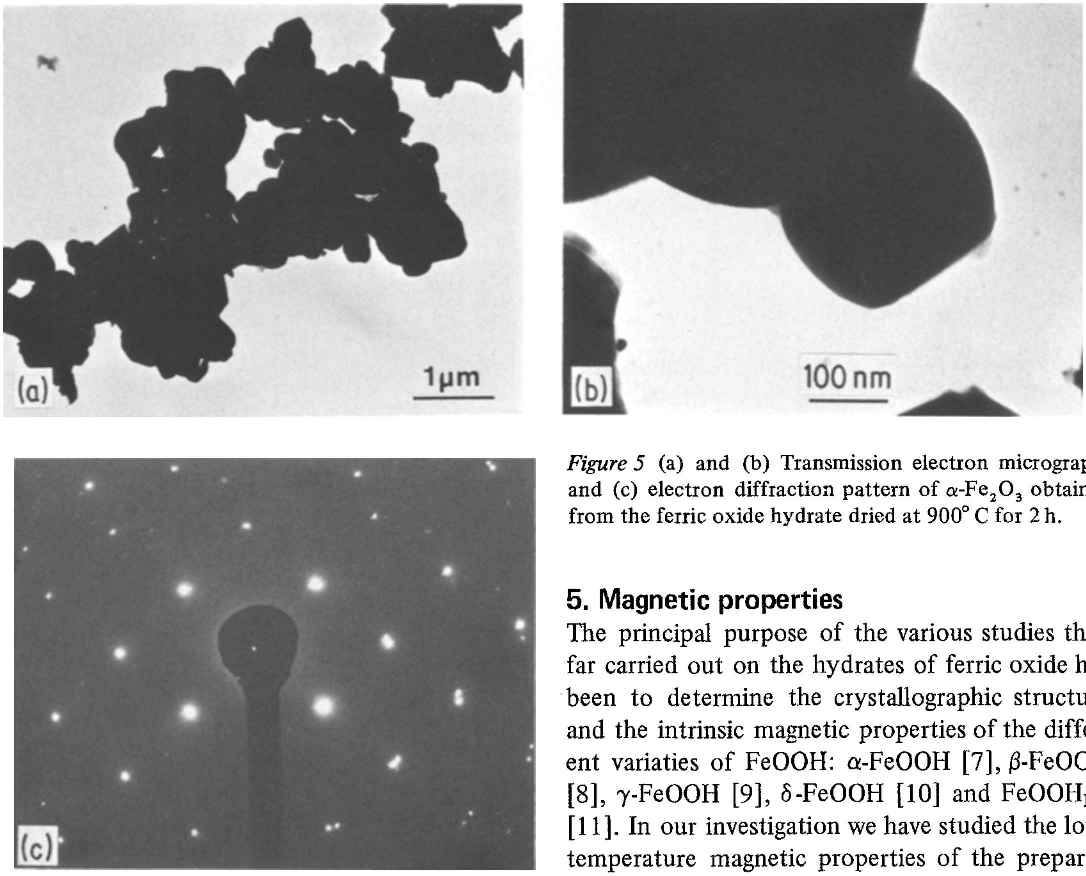

Figure 5 (a) and (b) Transmission electron micrographs and (c) electron diffraction pattern of α-Fe_2O_3 obtained from the ferric oxide hydrate dried at 900° C for 2 h.

$$\begin{aligned}&\alpha\text{-}Fe_2O_3 \rightarrow Fe_3O_4 \text{ (reduction under } H_2, 350^\circ\text{ C}, 0.5\text{ h)}\\ &Fe_3O_4 \rightarrow \gamma\text{-}Fe_2O_3 \text{ (re-oxidation in air, } 250^\circ\text{ C}, 0.5\text{ h).}\end{aligned} \quad (4)$$

To obtain crystallites of α-Fe_2O_3 larger than 10 nm, it would suffice to operate at a higher temperature during the thermal treatment. For example, annealing for 2 h at 900° C results in well-crystallized α-Fe_2O_3; the particle size can reach 100 nm (Fig. 5a). The electron diffraction pattern (Fig. 5c) corresponding to the same conditions under which the patterns seen in Figs 2c and 4c were obtained, is a single-crystal electron diffraction pattern, the crystals being much larger than in the two other cases. Besides, the lines which appear on the X-ray diffraction pattern (Fig. 1c) are much finer and more intense. They have the same appearance as those obtained from the commercial iron (III) oxide (Fig. 1d).

5. Magnetic properties

The principal purpose of the various studies thus far carried out on the hydrates of ferric oxide has been to determine the crystallographic structure and the intrinsic magnetic properties of the different variaties of FeOOH: α-FeOOH [7], β-FeOOH [8], γ-FeOOH [9], δ-FeOOH [10] and $FeOOH_{HP}$ [11]. In our investigation we have studied the low-temperature magnetic properties of the prepared ferric hydrate; these properties are essentially due to the very small size of the crystals.

5.1. Temperature dependence of magnetization

Curve a in Fig. 6 shows the variation of the magnetization, σ, ($H = 1.50 \times 10^6\,\mathrm{A\,m^{-1}}$) as a function of increasing temperature after the sample has been cooled without field down to 4.2 K. Curve b in Fig. 6 shows the variation of the magnetization ($H = 1.5 \times 10^6\,\mathrm{A\,m^{-1}}$) against T for decreasing temperature.

The non-reversibility of the magnetization variation can be explained by the magnetic properties of fine grains (12–14). Indeed, Curves a and b in Fig. 6 reveal a blocking temperature ($T_B \simeq 20$ K) for superparamagnetic grains. Ferric oxide hydrates generally present antiferromagnetic properties below a transition temperature lying above room temperature. At low temperature, the studied particles can consequently process a magnetic moment due to an imperfect compensation of moments of opposing directions [15]. Also, their relaxation time is very short becaue of their very small size, As a consequence, these ultrafine par-

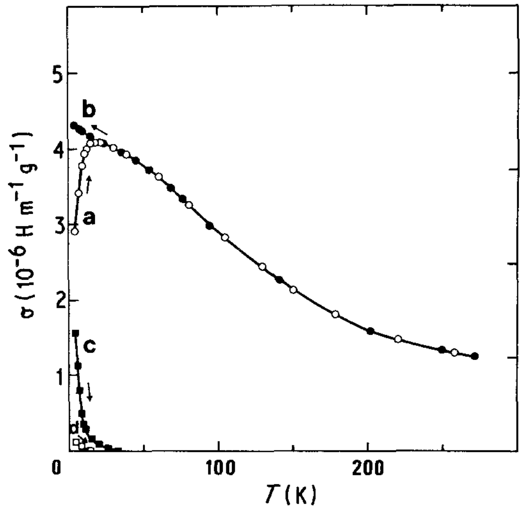

Figure 6 Magnetization against temperature data: variation of the magnetization ($H = 1.50 \times 10^6 \mathrm{A\,m^{-1}}$) as a function of (a) increasing temperature; (b) decreasing temperature; (c) TRM (thermoremanent magnetization); and (d) IRM (isothermal remanent magnetization).

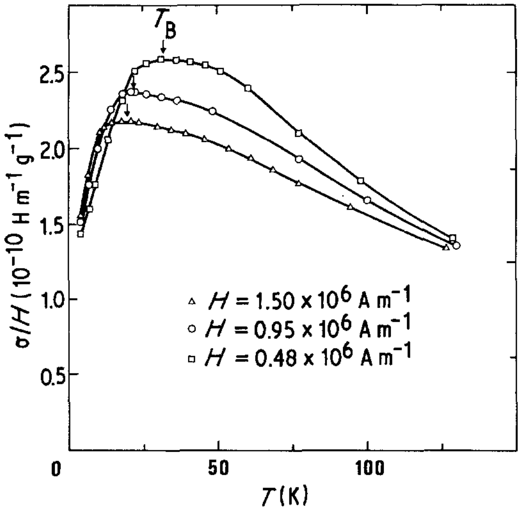

Figure 7 Field dependence of the blocking temperature, T_B.

ticles of ferric oxide hydrate are found to have superparamagnetic properties in the studied temperature range.

When superparamagnetic grains are cooled in a magnetic field below their blocking temperature, the magnetic moments of these particles are preferentially "frozen" with orientations closely parallel to the direction of the field. On the other hand, after zero-field cooling there is no preferential magnetization direction: net magnetization is equal to zero. When a magnetic field ($H = 1.50 \times 10^6 \mathrm{A\,m^{-1}}$) is then applied to this zero-field cooled sample, the magnetization (Curve a in Fig. 6) is lower than the one obtained from the sample which is cooled in the same magnetic field (Curve b in Fig. 6). This smaller value of magnetization is due to the grains which remain frozen in statistically random orientations despite the applied magnetic field. When the temperature increases, these grains relax and align themselves in directions closely parallel to the magnetic field, resulting in the magnetization increase appearing in Curve a in Fig. 6. As the relaxation time of grains is a function of their size (representing a certain dispersion), the thermic unblocking of the grains is progressive between 4.2 and 20 K, the "blocking temperature", for a magnetic field of $1.50 \times 10^6 \mathrm{A\,m^{-6}}$. Above this blocking temperature, where all the magnetic moments are unblocked, Curves a and b (in Fig. 6) coincide.

5.2. TRM and IRM study

The freezing of magnetic moments by field cooling leads, when the field is removed, to so-called thermoremanent magnetization (TRM). As the temperature increases, the magnetic moments relax and align themselves along the easy magnetization axes of the grains. At 35 K, because of the random orientation of the grains, the resulting magnetization is equal to zero (Curve c of Fig. 6). It might have been thought that this thermoremanent magnetization would be equal to zero at the previously determined "blocking temperature" of 20 K. In fact the relaxation time is a function of the applied field: the reorientation of the moments is all the more rapid as the magnetic field is higher (Fig. 7). When the field is equal to zero, the relaxation time is large and the TRM decreases slowly: its disappearance takes place at a higher temperature. One can finally note the classic curve of the TRM variation as a function of the field applied during the cooling (see Fig. 8).

The isothermal remanent magnetization (IRM) is much smaller than the TRM, and it becomes equal to zero at a relatively lower temperature (Curve d of Fig. 6).

5.3. Field dependence of the magnetization

Two studies of the prepared ferric oxide hydrate have been made at the temperature of liquid helium, one of a zero-field cooled sample, the other of a field cooled sample ($H = 1.50 \times 10^6 \mathrm{A\,m^{-1}}$).

As for the zero-field cooled sample, its magnet-

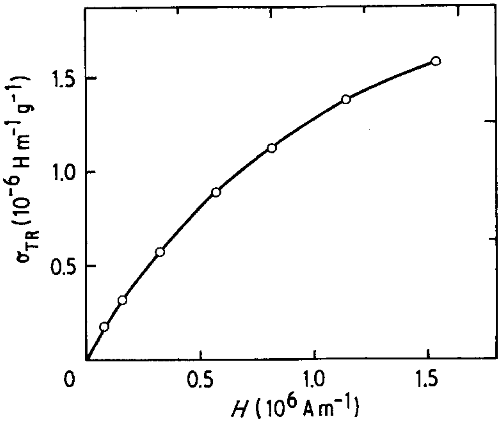

Figure 8 TRM variation as a function of the field applied during cooling to 4.2 K.

ization was measured resulting from an increase and then a decrease in the magnetic field (Curve a in Fig. 9). This magnetization is the result of two phenomena. Increasing field leads first to a progressive rotation of the magnetic moments which tend to align themselves with the magnetic field direction, resulting in a practically linear variation of magnetization. Between 0.80×10^6 and $1.50 \times 10^6 \mathrm{A\,m^{-1}}$ a second phenomenon appears in addition to the first: the magnetic moments which were frozen are reversed and tend to align themselves with the applied field. When the magnetic field decreases the magnetic moments return progressively to their zero-field equilibrium position, except those which have been reversed by the magnetic field. The result is a linear decrease of the magnetization and the appearance of an isothermal remanent magnetization.

In cooling the sample in a magnetic field of $1.50 \times 10^6 \mathrm{A\,m^{-1}}$, one obtains, after several cycles, a stable hysteresis loop (Curve b in Fig. 9) shifted along the magnetic moment axis of the diagram [16]. This translation corresponds to the TRM value. An identical, but symmetrical with respect to the origin, hysteresis loop can be obtained by turning the sample ($\theta = 90°$) so that the TRM direction is perpendicular to the magnetic field during the measurement.

The field dependence of magnetization was also studied at a number of temperatures above the blocking temperature. The obtained curves (Fig. 10) reveal superparamagnetic properties [17].

6. Discussion

The iron (III) oxide hydrate which has been prepared can be compred with the hydrates prepared and studied by certain authors, for instance van der Giessen [3, 17, 18], Okamoto [19] or Glemser [2].

Okamoto prepared an oxide hydrate with a water content ranging approximately from 22 to 15 wt% (21 wt% for our product): a ferric nitrate solution was added into a sodium hydroxide solution (0.1 N to 10 N) at 20° C, and the precipitate was dried in vacuum over P_2O_5 at room temperature. van der Giessen obtained iron (III) oxide hydrates by hydrolysis of ferric nitrate in aqueous solutions [18] and by treating a solution of ferric nitrate with concentrated ammonia [3].

Electron micrographs revealed in these different cases that the gel of hydrate consists of extremely small particles with a diameter of several nano-

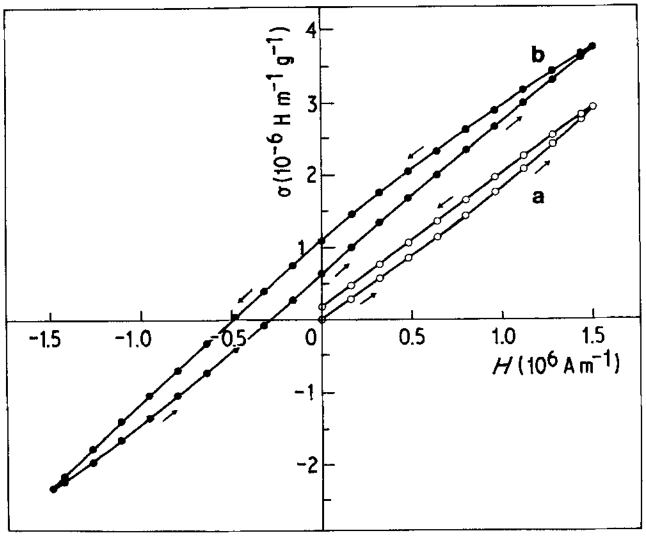

Figure 9 Magnetization against field plots at 4.2 K of (a) a zero-field cooled sample and (b) a field ($H = 1.5 \times 10^6 \mathrm{A\,m^{-1}}$) cooled sample.

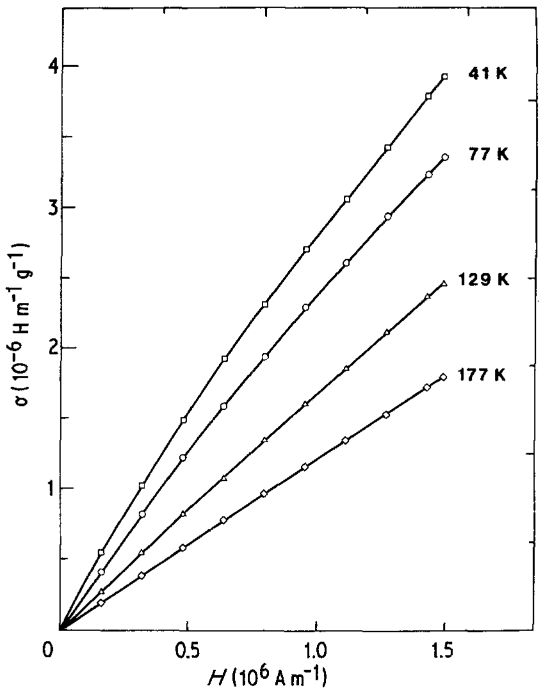

Figure 10 Magnetization against field plots at temperatures above the blocking temperature.

metres. Particles were observed of size less than 2 nm.

Thermogravimetric and differential thermal analysis allowed van der Giessen to show that the dehydration (20 to 200° C) and the recrystallization (350 to 450° C) are separate processes. These data are similar to those obtained in this work: thermogravimetry revealed that the dehydration of the hydrate is preactically complete at 250° C and an X-ray diffraction study with temperature showed a crystallization of α-Fe_2O_3 from 300° C.

Van der Giessen and Okamoto could obtain X-ray diagrams of the iron oxide hydrates they prepared. On the contrary, no line can be seen in the X-ray pattern of our hydrate constituted of smaller particles. Nevertheless, two diffraction rings appear in the electron diffraction pattern, indicating a certain degree of crystallinity. The d-spacings for these two diffraction circles (Fig. 2c) are, respectively, equal to 0.265 nm and 0.154 nm. They present a certain analogy with the X-ray data of both authors: for the two strongest reflections, van der Giessen gives $d \simeq 0.252$ nm and $d \simeq 0.149$ nm [18]; Okamoto proposes 0.254 nm and 0.147 nm [19].

The magnetization values of the iron (III) oxide hydrates prepared by both authors in an alkaline solution are higher than these measured in the present work. van der Giessen gives a value of about 9×10^{-4} T cm^3 g^{-1} at 4.2 K for a magnetic field of 1.51×10^6 A m^{-1} [3]. In the same conditions of field and temperature, the hydrate which we have not prepared in an alkaline solution has a magnetization of about 3.8×10^{-6} H m^{-1} g^{-1}. This result is in accordance with the magnetic study realised by Okamoto who showed that the magnetization value was higher when the ferric hydroxide gel was precipitated in a solution of higher NaOH concentration. At 4.2 K and in a field of 0.80×10^6 A m^{-1} the magnetization ranges from 5×10^{-4} T cm^3 g^{-1} (NaOH 0.1 N) to 2×10^{-3} T cm^3 g^{-1} (NaOH 10 N). Okamoto and van der Giessen also examined the superparamagnetic properties of their hydrates, with particular attention given to the region above the blocking temperature.

7. Conclusion

The magnetic study of the ferric oxide hydrate, prepared in this work, very clearly allowed the demonstration of phenomena which are characteristic, but relatively unknown, of fine grains. These properties (superparamagnetism, blocking temperature and thermoremanent magnetization) were observed for the first time in studying fine grains. They have also been shown to appear in more recently studied mictomagnetic compounds [20], particularly in some alloys [21] and magnetic glasses [22]. This analogy can be explained by the presence, in these mictomagnetic materials, of clusters with "giant magnetic moments" the behaviour of which resembles that of the magnetic moments of fine grains.

Acknowledgements

The authors are grateful to G. Ehret, and Professor J. P. Eberhart of Laboratoire de Minéralogie de Strasbourg for the micrographs.

References

1. P. L. GUNTHER and H. REHAAG, *Z. anorg. allg. Chem.* 243 (1939) 60.
2. O. GLEMSER and G. RIECK, *ibid.* 297 (1958) 175.
3. A. A. VAN DER GIESSEN, *J. Inorg, Nucl. Chem.* 28 (1966) 2155.
4. H. B. WEISER and W. O. MILLIGAN, *J. Phys. Chem.* 44 (1940) 1081.
5. K. HANEDA and A. H. MORRISH, *Sol. Stat. Comm.* 22 (1977) 779.
6. S. HAMADA and K. KUMA, *Bull. Chem. Soc. Japan* 50 (1977) 1635.

7. A. SZYTULA, A. BUREWICZ, Z. DIMITRIJEVIC, S. KRASNICKI, H. RZANY, J. TODOROVIC, A. WANIC and W. WOLSKI, *Phys. Status Solidi* **26** (1968) 429.
8. A. SZYTULA, M. BALANDA and Z. DIMITRIJEVIC, *Phys. Status Solidi (A)* **3** (1970) 1033.
9. A. OLES, A. SZYTULA and A. WANIC, *Phys. Status Solidi* **41** (1970) 173.
10. W. KRAKOW, H. COLIJN and O. MULLER, *J. Mater. Sci.* **15** (1980) 119.
11. M. PERNET, J. C. JOUBERT and C. BERTHET-COLOMINAS, *Sol. Stat. Comm.* **17** (1975) 1505.
12. L. NEEL, *Ann. Géophys.* **5** (1949) 99.
13. *Idem, J. Phys. Soc. Japan* **17** Suppl. B-1 (1962) 676.
14. C. P. BEAN and J. D. LIVINGSTON, *J. Appl. Phys.* **30** Suppl. 4 (1959) 120.
15. *Idem, Compt. Rend.* **252** (1961) 4075.
16. J. COHEN, K. M. CREER, R. PAUTHENET and K. SRIVASTAVA, *J. Phys. Soc. Japan* **17** Suppl. B-1 (1962) 685.
17. A. A. VAN DER GIESSEN, *J. Phys. Chem. Sol.* **28** (1967) 343.
18. *Idem, Philips Res. Repts. Suppl. Number 12* (1968) 1.
19. S. OKAMOTA, H. SEKIZAWA and S. I. OKAMOTO, Proceedings of the 7th International Symposium on the Reactivity of Solids, edited by J. S. Anderson, M. W. Roberts, F. S. Stone (Chapman and Hall, London, 1972) p. 341.
20. P. A. BECK, *Prog. Mater. Sci.* **23** (1978) 1.
21. *Idem, Met. Trans.* **2** (1971) 2015.
22. H. LAVILLE and J. C. BERNIER, *J. Mater. Sci.* **15** (1980) 73.

Received 3 February
and accepted 15 July 1981